Inorg. Chem. **1988**, *27*, 4355-4361

absorption spectra in SO_2 showed bands at 475 nm (I_3^+) and 648 nm (I_2^+). Because of strong absorption by SO_2, bands below 350 nm could not be observed.

Gillespie et al. have reported that solutions of I_2^+ in HSO_3F change from the characteristic deep blue color of I_2^+ at room temperature to a red-brown color at -80 °C.[6] They showed by a combination of magnetic, cryoscopic, and conductometric measurements that I^{2+} dimerizes to I_4^{2+} at low temperature. In the present investigation, we have studied Raman spectra of a solution of $I_2^+(Sb_2F_{11}^-)$ in HSO_3F as a function of temperature (Figure 4). Between room temperature and -60 °C, the spectra showed only the characteristic peak of I_2^+ at 238 cm^{-1}.[29] At lower temperatures, however, as the color of the solution changed from blue to red, a new peak appeared at 232 cm^{-1} and the 238-cm^{-1} peak decreased in intensity. The first overtone of each peak was observed at 464 and 476 cm^{-1}, respectively. At -120 °C, the 232-cm^{-1} peak was much stronger than the 238-cm^{-1} peak, indicating that the dimerization was essentially complete.

Acknowledgment. We wish to thank the Natural Sciences and Engineering Research Council of Canada for operating grants.

Registry No. **1**, 84493-41-4; **2**, 117041-29-9; **3**, 117041-30-2; I_2, 7553-56-2; AsF_5, 7784-36-3; SbF_5, 7783-70-2; $I_2Sb_2F_{11}$, 53108-64-8; NaF, 7681-49-4.

Supplementary Material Available: For **1**–**3**, Tables A–C (anisotropic temperature factors) (2 pages); tables of observed and calculated structure factors (45 pages). Ordering information is given on any current masthead page.

Contribution from the Department of Chemistry, The Pennsylvania State University, University Park, Pennsylvania 16802,
Union Carbide Corporation, South Charleston, West Virginia 25303,
and Department of Chemistry, The University of Delaware, Newark, Delaware 19716

Equilibria within the $Ru_3(CO)_{12}$/Halide System

Sung-Hwan Han,[†] Gregory L. Geoffroy,[*,†] B. Duane Dombek,[*,‡] and Arnold L. Rheingold[§]

Received May 9, 1988

The results reported herein, when combined with those from earlier studies, present a comprehensive picture of the various equilibria that exist in $Ru_3(CO)_{12}$ solutions containing halide ions. A remarkable number of complexes have been found to form and interconvert, with the position of the equilibria dependent upon temperature, the CO partial pressure, and the specific halide employed. All experiments described herein have used the $[(Ph_3P)_2N]^+$ halide salts, except as noted. As previously noted by Kaesz and co-workers, $Ru_3(CO)_{12}$ rapidly reacts with Cl^- and Br^- ions to initially form the clusters $[Ru_3(X)(CO)_{11}]^-$ (**2a,b**), which reversibly lose CO to produce the species $[Ru_3(\mu_2\text{-}X)(CO)_{10}]^-$ (**3a,b**). The reaction of $Ru_3(CO)_{12}$ with iodide proceeds immediately to form $[Ru_3(\mu_2\text{-}I)(CO)_{10}]^-$ (**3c**) but with no evidence for the intermediacy of a cluster analogous to **2a** and **2b**. Clusters **3a** and **3b** rapidly add CO at 1 atm to form **2a** and **2b**, but cluster **3c** does not take up CO under these mild conditions. When heated, the trinuclear clusters **3a–c** all lose CO to transform reversibly into other species, but with the final product dependent upon the halide. The chloro and bromo derivatives **3a** and **3b** form the tetranuclear butterfly clusters $[Ru_4(\mu_2\text{-}X)(CO)_{13}]^-$ (**6a** and **6b**), along with $^1/_4$ equiv of halide ion, and these reactions are cleanly reversed by placing **6a** and **6b** with the necessary halide under 1 atm of CO. The iodo cluster **3c** loses CO upon heating to form the trinuclear species $[Ru_3(\mu_3\text{-}I)(CO)_9]^-$ (**7c**), which has been crystallographically defined as the $[Na(18\text{-crown-}6)]^+$ salt: space group *Pnma*, $a = 20.214$ (5) Å, $b = 21.592$ (6) Å, $c = 15.199$ (3) Å, $V = 6634$ (2) Å^3, $Z = 8$, $R(F) = 7.92\%$, $R_w(F) = 8.92\%$ for 2879 reflections with $F_o \geq 4\sigma F_o$. The triangular metal core of **7c** is symmetrically capped by a μ_3-iodide ligand. Each Ru atom has two terminal CO's, and CO ligands bridge each of the Ru–Ru bonds. Cluster **7c** can be reversibly protonated to form the known species $HRu_3(\mu_3\text{-}I)(CO)_9$. Cluster **7c** also rapidly forms upon reaction of **3c** with H_2O, a reaction that also produces CO_2 and H_2, and **3c** is a catalyst for the water gas shift reaction. When the reaction of $Ru_3(CO)_{12}$ with iodide was conducted under an H_2/CO atmosphere, disproportionation occurred to form $[HRu_3(CO)_{11}]^-$ and $[RuI_3(CO)_3]^-$. A similar reaction occurred when cluster **7c** was placed under H_2. Cluster **7c** has also been found to thermally decompose to form $[Ru_6(CO)_{18}]^{2-}$ when heated to 100 °C. However, at 140 °C, **7c** forms the carbide cluster $[Ru_6C(CO)_{16}]^{2-}$. The reaction of $Fe_3(CO)_{12}$ with iodide has been reinvestigated and found to produce $[Fe(CO)_4I]^-$ along with small amounts of $[HFe_3(CO)_{11}]^-$ that form from traces of water.

Introduction

Halides are highly effective promoters of a number of reactions catalyzed by $Ru_3(CO)_{12}$,[1-5] but the role of the halide is in general poorly understood. The one catalytic reaction that has been most thoroughly studied from a phenomenological perspective is the halide-promoted formation of methanol, ethylene glycol, and acetic acid from synthesis gas.[1-3] It is known that significant rate enhancements and altered selectivities are provided in these systems by halides, but a full understanding of the roles of these promoters has yet to be developed. It is known, however, that the catalytic solutions in these reactions often contain ruthenium halide complexes and anionic clusters. One role of the halides may be to stabilize complexes in the catalytically important oxidation states.[6]

To understand the promoting role of halide on $Ru_3(CO)_{12}$ catalysis, it is essential to understand first the basic reactions that occur when halides react with $Ru_3(CO)_{12}$. Kaesz and his coworkers have provided an important insight in this area through their demonstration that halides stoichiometrically react with $Ru_3(CO)_{12}$ to form the anionic clusters **3a–c**, (Scheme I).[7] These complexes were further shown to yield the neutral hydride clusters **4a–c** upon protonation, and it was also reported that complex **4c** reversibly loses CO to form the cluster **5c** with a triply bridging iodide ligand.[8] Spectroscopic data have been reported for complexes **3a**, **4a–c**, and **5c**. Furthermore, complexes **4b** and **5c** have been fully defined by X-ray diffraction studies.[8] The use of LiX salts coupled with Me_3NO as a carbonyl labilizer was originally used to induce the formation of **3a–c**, but such reaction gave only

---

[†] The Pennsylvania State University.

[‡] Union Carbide Corp.

[§] University of Delaware.

(1) (a) Dombek, B. D. *J. Organomet. Chem.* **1983**, *250*, 467. (b) Dombek, B. D. *J. Am. Chem. Soc.* **1981**, *103*, 6508. (c) Dombek, B. D. *Eur. Pat. Appl.* **1979**, 0013008. (d) Dombek, B. D. *Organometallics* **1985**, *4*, 1707.

(2) (a) Knifton, J. F. *J. Am. Chem. Soc.* **1981**, *103*, 3959. (b) Knifton, J. F. *J. Mol. Catal.* **1981**, *11*, 91.

(3) Yoshida, S. I.; Mori, S.; Kinoshita, H.; Watanabe, Y. *J. Mol. Catal.* **1987**, *42*, 215.

(4) Hidai, M.; Koyasu, Y.; Chikanari, K.; Uchida, Y. *J. Mol. Catal.* **1987**, *40*, 243.

(5) Cenini, S.; Pizoti, M.; Crotti, C.; Porta, F.; Monica, G. L. *J. Chem. Soc., Chem. Commun.* **1985**, 241.

(6) Dombek, B. D. *Comments Inorg. Chem.* **1985**, *4*, 241.

(7) Lavigne, G.; Kaesz, H. D. *J. Am. Chem. Soc.* **1984**, *106*, 4647.

(8) Kampe, C. E.; Boag, N. M.; Knobler, C. B.; Kaesz, H. D. *Inorg. Chem.* **1984**, *23*, 1390.

0020-1669/88/1327-4355$01.50/0

Scheme I

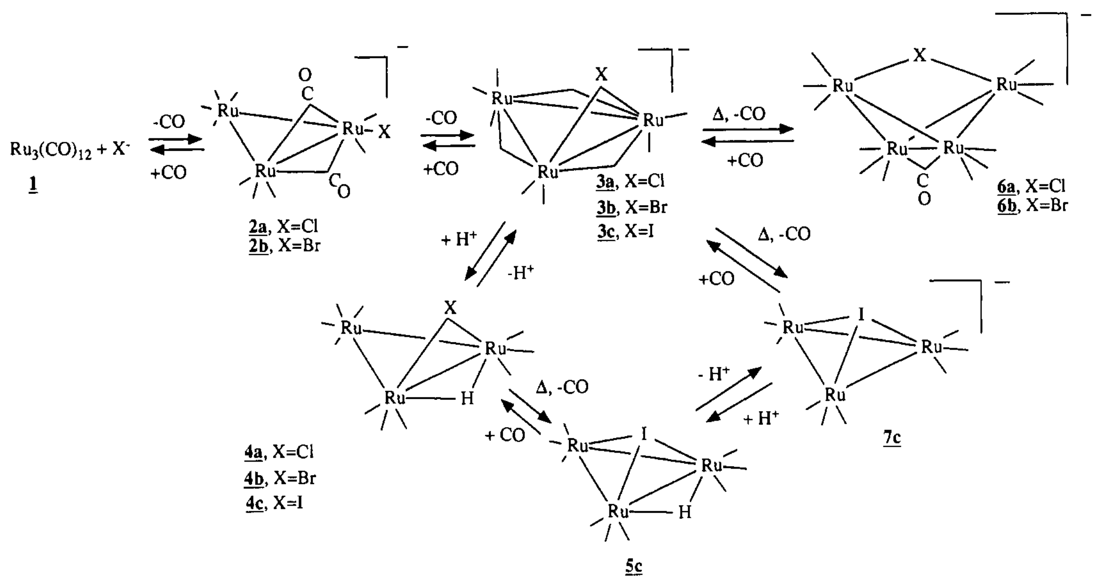

modest yields of **3** and **4**, apparently due to the low solubility of the lithium halide in THF. Kaesz later noted that the more soluble [PPN]Cl [PPN = $(Ph_3P)_2N^+$] in THF gave a nearly quantitative yield of **3** without the use of Me_3NO.[7] These workers also noted that small quantities of halides catalyze substitution reactions of $Ru_3(CO)_{12}$, and a discussion of how that may occur is given by Kaesz and Lavigne in ref 9.

In related work, one of us had earlier shown that the reaction of $Ru_3(CO)_{12}$ with [PPN]Cl in *refluxing* THF, instead of at room temperature as in Kaesz's studies, gave high-yield formation of the tetranuclear butterfly cluster **6a** (eq 1).[10a] However, it has never been shown whether the ambient- and elevated-temperature reactions are connected and whether or not complexes **3a** and **6a** can be interconverted. Furthermore, comparable elevated-temperature reactions of $Ru_3(CO)_{12}$ with [PPN]Br and [PPN]I have not been described.

$$4Ru_3(CO)_{12} + 3[PPN]Cl \xrightarrow[1\,h,\,THF]{57\,°C}$$

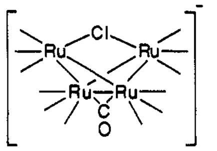

(1)

6a (50%)

In the course of various studies on chemistry within the $Ru_3(CO)_{12}$/halide system in our two independent laboratories,[1,10] a more comprehensive picture of the equilibria present within these systems has emerged, and those results are described herein. The various equilibria that are present in the $Ru_3(CO)_{12}$/halide system, as deduced from earlier work and from the studies described herein, are shown in Scheme I. The new compounds described in this study are clusters **6b** and **7c**, although spectroscopic data are reported for the first time for **2a–b** and **3b–c**. Cluster **7c** has been fully characterized by an X-ray diffraction study. Also described are related reactions of $Ru_3(CO)_{12}$ with iodide under H_2/CO atmospheres and comparable reactions of $Fe_3(CO)_{12}$ with iodide.

Results

Ambient-Temperature Reaction of $Ru_3(CO)_{12}$ with Halides. As previously noted by Kaesz and co-workers,[7,8] the [PPN]X salts react with $Ru_3(CO)_{12}$ over a 1–2-h period in THF solution at 22 °C. However, the rates of the reactions appear to be limited only by the rate at which the [PPN]X salt dissolves in the solvent, and they were complete within minutes when CH_2Cl_2 *solutions* of the [PPN]X salts were added to solutions of $Ru_3(CO)_{12}$. The exact positions of the various equilibria present (Scheme I) depend markedly upon the CO pressure and the halide employed. For X = Cl and Br, when the reactions were conducted in the absence of excess CO in a closed vessel, they proceeded initially to form clusters **2a** and **2b**, but when the released CO was removed by an N_2 purge or by solvent evaporation, the decacarbonyl clusters **3a** and **3b** were quantitatively formed. These reactions immediately and quantitatively reversed to form **2a** and **2b** when clusters **3a** and **3b** were placed under 1 atm CO. No evidence was obtained for an iodo cluster analogous to **2a** and **2b** in the reaction of [PPN]I with $Ru_3(CO)_{12}$. At ambient temperature, this reaction proceeded initially to form cluster **3c**. This latter species is stable under 1 atm CO and does not form a cluster analogous to **2a** under these conditions.

The decacarbonyl clusters **3** were each isolated as microcrystalline solids, although they were difficult to obtain in pure form because of their tendency to lose CO (see below). Cluster **3a** with X = Cl^- has been well characterized by Kaesz and co-workers[7] and presumably has the structure shown in Scheme I since a similar structure has been established for $[Ru_3(\mu\text{-}O_2CH)(CO)_{10}]^-$, which has an IR spectrum very similar to that of **3a**.[11] The structures of the bromo and iodo analogues must be similar to that of **3a** since the IR spectral data of all three clusters (Table I) are nearly identical. Although clusters **3b** and **3c** have not been previously characterized, they were obvious intermediates in Kaesz's preparations of the corresponding well-defined hydride derivatives $HRu_3(\mu\text{-}X)(CO)_{10}$.[8]

Clusters **2** cannot be isolated because of the facility with which they lose CO to form **3**. We have characterized each in situ by their IR spectral data (Table I). Other workers[12,13a] have suggested that these species have the structure shown in Scheme I, consistent with the presence of bridging carbonyl bands in their IR spectra. An analogous X = NCO^- derivative has been spectroscopically characterized by Gladfelter and co-workers.[13b]

Interconversion of the Trinuclear Clusters 3a and 3b with the Tetranuclear Clusters 6a and 6b. Although solutions of the decacarbonyl clusters **3a** and **3b** were stable for several hours at ambient temperature under N_2, slow conversion to the tetranuclear clusters $[Ru_4(\mu_2\text{-}X)(CO)_{13}]^-$ (**6a**, X = Cl; **6b**, X = Br) occurred

---

[9] Lavigne, G.; Kaesz, H. D. In *Metal Clusters in Catalysis*; Knozinger, H., Gates, B. C., Guczi, L., Eds.; Elsevier: Amsterdam, 1986; pp 68–69.

[10] (a) Steinmetz, G. R. Harley, D.; Goeffroy, G. L. *Inorg. Chem.* **1980**, *19*, 2985. (b) Han, S. H.; Geoffroy, G. L.; Rheingold, A. L. *Inorg. Chem.* **1987**, *26*, 3428. (c) Morrison, E.; Geoffroy, G. L. *J. Am. Chem. Soc.* **1985**, *107*, 3541.

[11] Darensbourg, D. J.; Pala, M.; Walker, J. *Organometallics* **1983**, *2*, 1285.

[12] Lavigne, G.; Lugan, N.; Bonnet, J. J. *J. Chem. Soc., Chem. Commun.* **1987**, 957.

[13] (a) Gladfelter, W. L., personal communication. (b) Fjare, D. E.; Jensen, J. A.; Gladfelter, W. L. *Inorg. Chem.* **1983**, *22*, 1774.

Table I. IR Data

compd	ν(CO), cm^{-1}
$Ru_3(CO)_{12}$ (**1**)[a]	2062 (vs), 2029 (m), 2011 (m)
[PPN][$Ru_3(Cl)(CO)_{11}$] (**2a**)[a]	2099 (w), 2060 (m), 2026 (vs), 2010 (s), 1978 (sh), 1960 (w), 1829 (m)
[PPN][$Ru_3(Br)(CO)_{11}$] (**2b**)[a]	2059 (m), 2026 (vs), 2008 (s), 1993 (m), 1973 (sh), 1963 (sh), 1829 (m)
[PPN][$Ru_3(\mu_2\text{-}Cl)(CO)_{10}$] (**3a**)[a]	2070 (m), 2026 (m), 1993 (vs), 1981 (m), 1954 (m), 1907 (w), 1800 (m), 1771 (w)
[PPN][$Ru_3(\mu_2\text{-}Br)(CO)_{10}$] (**3b**)[a]	2070 (w), 2026 (m), 1991 (vs), 1952 (m), 1908 (m), 1800 (m), 1773 (w)
[PPN][$Ru_3(\mu_2\text{-}I)(CO)_{10}$] (**3c**)[a]	2083 (w), 2070 (w), 2024 (s), 1993 (s), 1977 (sh), 1956 (sh), 1802 (w)
$HRu_3(\mu_2\text{-}Cl)(CO)_{10}$] (**4a**)[b]	2113 (vw), 2077 (w), 2070 (s), 2034 (sh), 2030 (vs), 1997 (w)
$HRu_3(\mu_2\text{-}Br)(CO)_{10}$ (**4b**)[b]	2112 (w), 2076 (s), 2069 (s), 2030 (vs), 2024 (sh), 1996 (w)
$HRu_3(\mu_2\text{-}I)(CO)_{10}$ (**4c**)[b]	2108 (w), 2077 (s), 2069 (m), 2030 (vs), 2019 (w), 1996 (w)
$HRu_3(\mu_3\text{-}I)(CO)_9$ (**5c**)[a]	2096 (w), 2070 (vs), 2049 (s), 2017 (vs), 1988 (w)
[PPN][$Ru_4(\mu_2\text{-}Cl)(CO)_{13}$] (**6a**)[a]	2070 (w), 2027 (m), 2006 (s), 1970 (m), 1958 (m), 1838 (w)
[PPN][$Ru_4(\mu_2\text{-}Br)(CO)_{13}$] (**6b**)[c]	2060 (w), 2028 (s), 2004 (vs), 1975 (m), 1960 (m), 1830 (w), 1750 (w)
[PPN][$Ru_3(\mu_3\text{-}I)(CO)_9$] (**7c**)[c]	2042 (w), 2037 (w), 1997 (vs), 1958 (s), 1793 (m)
[PPN][$HRu_3(CO)_{11}$] (**8**)[a]	2072 (w), 2016 (vs), 1992 (vs), 1954 (m), 1710 (w)
[PPN][$RuI_3(CO)_3$] (**9**)[c]	2102 (s), 2033 (s)
$[PPN]_2[Ru_6(CO)_{18}]$ (**10**)[c]	2003 (s), 1990 (vs), 1938 (w), 1915 (w, sh), 1765 (w)
$[PPN]_2[Ru_6C(CO)_{16}]$ (**11**)[c]	2032 (w), 1984 (vs), 1955 (m, sh), 1920 (m), 1820 (m, sh), 1785 (m)
[PPN][$FeI(CO)_4$] (**12**)[a]	2018 (m), 1948 (w), 1921 (s)
[PPN][$Fe_3(\mu_2\text{-}H)(CO)_{11}$] (**13**)[a]	2061 (w), 2000 (vs), 1979 (m), 1957 (m), 1944 (m), 1752 (w)

[a] THF solution. [b] Reference 8; hexane solution. [c] CH_2Cl_2 solution.

over the course of several days. These latter reactions were accelerated by heating and proceeded in nearly quantitative yield in refluxing THF solution. Cluster **6a** has been previously characterized by a crystal structure analysis.[10a] The bromide derivative **6b** has an IR spectrum similar to that of **6a** (Table I), indicating similar butterfly structures for the two compounds.

The tetranuclear clusters **6a** and **6b** also rapidly react with CO (1 atm, 22 °C, ~20 min) to form the trinuclear clusters **2a** and **2b**, reactions that logically proceed via the intermediacy of **3a** and **3b**. When pure **6a,b** was exposed to CO, $^1/_3$ equiv of $Ru_3(CO)_{12}$ was also produced (eq 2) since insufficient halide was present for

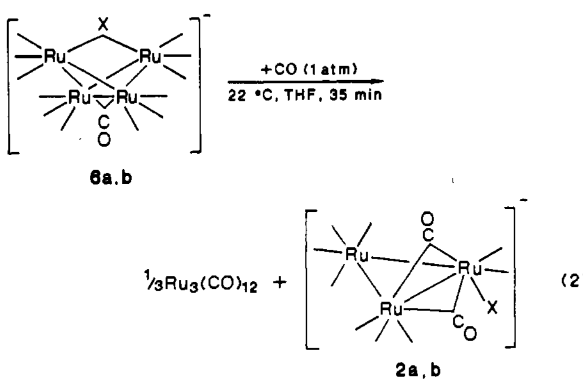

quantitative conversion to **2a,b**. However, when solutions of **6a,b** that were generated by the sequence of reactions shown in Scheme I were placed under 1 atm of CO, clusters **2a,b** were quantitatively produced since these solutions contained the necessary $^1/_2$ equiv of halide for complete reaction.

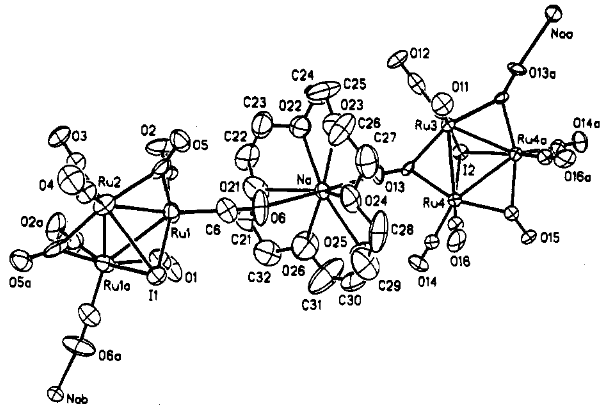

Figure 1. Structure and labeling scheme for [Na(18-crown-6)][$Ru(\mu_3\text{-}I)(CO)_9$]·$0.5CH_2Cl_2$ (**7c**). The solvent molecule and hydrogen atoms have been omitted for clarity; thermal ellipsoids are drawn with 40% probability contours. The Na atoms Na(a) and Na(b) are included to indicate the zigzag, one-dimensional array of ionic components. The unit cell contains two independent cluster anions.

Scheme II

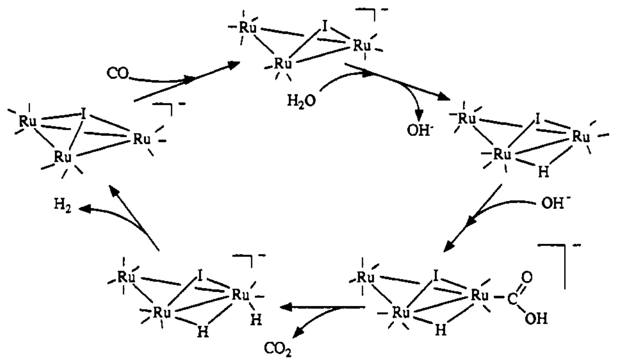

Interconversion of the Trinuclear Clusters 3c and 7c. When solutions of the iodo cluster **3c** were heated, a tetranuclear derivative similar to **6a** and **6b** did not form, but instead the cluster lost CO and the trinuclear species **7c** with a triply bridging iodide ligand was produced. This latter cluster was isolated as an orange crystalline solid and has been crystallographically characterized (Figure 1, see below). As indicated in Scheme I, this species smoothly protonates to form the cluster $HRu_3(\mu_3\text{-}I)(CO)_9$ (**5c**),[8] which was previously characterized by Kaesz and co-workers. The latter cluster can in turn be deprotonated by Et_3N to re-form **7c**. When placed under 1 atm of CO, cluster **7c** rapidly takes up CO to quantitatively form **3c**, and the **3c** ⇌ **7c** interconversion can be repeatedly cycled without loss of complex.

Reaction of $[Ru_3(\mu_2\text{-}I)(CO)_{10}]^-$ with H_2O. Catalysis of the Water Gas Shift Reaction. The iodo cluster **3c** cleanly reacts with water over the course of several hours at 22 °C to form cluster **7c** (eq 3). The carbon dioxide product of this reaction was

$$[Ru_3(\mu_2\text{-}I)(CO)_{10}]^- + H_2O \xrightarrow[\text{THF, 4h}]{22\ °C} [Ru_3(\mu_3\text{-}I)(CO)_9]^- + CO_2 + H_2 \quad (3)$$

identified by mass and IR analysis. Although the formation of H_2 was not proven, it is the logical product of this transformation. Since cluster **7c** rapidly reacts with CO to form cluster **3c** (Scheme I), this system exhibits all the necessary reaction steps to complete a catalytic cycle for the water gas shift reaction. Such catalysis does indeed occur, but with a relatively low turnover number of about 5/day/Ru at 100 °C and 50 psi of CO. A possible catalytic cycle, based on the individual reaction steps demonstrated herein, is shown in Scheme II. Catalysis of the water gas shift reaction by basic $Ru_3(CO)_{12}$ solutions in the absence of halide has been well studied.[14]

Reaction of $Ru_3(CO)_{12}$ with Iodide in the Presence of H_2. When THF solutions of $Ru_3(CO)_{12}$ and [PPN]I were allowed to react at elevated temperatures under H_2 or H_2/CO atmospheres instead of N_2 atmospheres as above, cluster **7c** was not formed, but instead a different set of reaction products was observed. Hydrogen activation occurred, and a disproportionation process gave the two ruthenium complexes shown in eq 4. The known compounds **8**[15]

$$\tfrac{7}{3}\underset{\mathbf{1}}{Ru_3(CO)_{12}} + H_2 + 3I^- \xrightarrow[\text{3 atm of } H_2/CO]{\text{THF, 65 °C}} 2\underset{\mathbf{8}}{[HRu_3(CO)_{11}]^-} + \underset{\mathbf{9}}{fac\text{-}[RuI_3(CO)_3]^-} + 3CO \tag{4}$$

and **9**[16] were observed by IR spectroscopy, and they were also individually isolated from the reaction mixture. The reactions described in the above paragraph show that $Ru_3(CO)_{12}$ reacts rapidly with iodide to form the trinuclear clusters **3c** and **7c**, and these species are logical intermediates in reaction 4. Indeed, when solutions of **7c** were exposed to H_2/CO, compounds **8** and **9** were formed (eq 5). The mechanisms of these processes are not entirely understood, but further experiments have suggested a plausible reaction pathway for the $Ru_3(CO)_{12}$ conversion. This complex reacts with H_2 in the presence of a base such as triethylamine to afford good yields of $[HRu_3(CO)_{11}]^-$ (eq 6) by a process that apparently involves formation of the intermediate $H_2Ru_3(CO)_{11}$ and its subsequent deprotonation by Et_3N.[15b] A number of experiments have shown that halide ions are sufficiently strong bases *in non-aqueous solvents* to deprotonate metal hydride complexes.[7,17] For example, both $H_4Ru_4(CO)_{12}$[7] and $HCoRu_2(\mu_3\text{-}NPh)(CO)_9$[17] undergo clean deprotonation when treated with [PPN]Cl in THF solution. Thus, $[HRu_3(CO)_{11}]^-$ could form via deprotonation of the intermediate $H_2Ru_3(CO)_{11}$ by iodide ion. It could also be produced by addition of H_2 to $[Ru_3(\mu_2\text{-}I)(CO)_{10}]^-$ (**3c**) to form $[H_2Ru_3(I)(CO)_{11}]^-$, which could then eliminate HI and add CO.

$$3\underset{\mathbf{7c}}{[Ru_3(\mu_3\text{-}I)(CO)_9]^-} + H_2 + 12CO \xrightarrow[\text{3 atm of } H_2/CO]{\text{THF, 65 °C}} 2[HRu_3(CO)_{11}]^- + [RuI_3(CO)_3]^- + \tfrac{2}{3}Ru_3(CO)_{12} \tag{5}$$

$$Ru_3(CO)_{12} + H_2 + Et_3N \xrightarrow[\text{1 atm of } H_2]{\text{THF, 65 °C}} [Et_3NH]\underset{\mathbf{8}}{[HRu_3(CO)_{11}]} + CO \tag{6}$$

The formation of $[RuI_3(CO)_3]^-$ is obviously a more complicated process, but it may proceed via the reaction of **3c** or **7c** with the HI released in the reaction described above. Indeed, we have observed that iodide solutions of $Ru_3(CO)_{12}$, which form **3c** and **7c**, react with HI according to eq 7.

$$\tfrac{1}{3}Ru_3(CO)_{12} + 2\,HI + I^- \xrightarrow[N_2]{\text{THF, 25 °C}} \underset{\mathbf{9}}{fac\text{-}[RuI_3(CO)_3]^-} + CO + H_2 \tag{7}$$

Thermolysis of $[Ru_3(\mu_3\text{-}I)(CO)_9]^-$ To Form $[Ru_6(CO)_{18}]^{2-}$ and $[Ru_6C(CO)_{16}]^{2-}$. When mixtures of $Ru_3(CO)_{12}$ and iodide salts or solutions of $[Ru_3(\mu_3\text{-}I)(CO)_9]^-$ (**7c**) were heated under N_2 to temperatures of approximately 120 °C, redox reactions occurred, and the major ruthenium-containing product isolated in good yield was $[Ru_6(CO)_{18}]^{2-}$ (eq 8). This complex was originally prepared by reduction of $Ru_3(CO)_{12}$ with $[Mn(CO)_5]^-$ in refluxing THF,[18a] and it has also been obtained by the reduction of $Ru_3(CO)_{12}$ with aqueous KOH in THF.[18b] Although iodine is liberated by the related iodide ion reduction of an Os(0) precursor to $[Os_6(CO)_{18}]^{2-}$,[19] there is no evidence for free iodine in the ruthenium reactions. It appears instead that oxidized ruthenium complexes containing iodide ligands are produced by a disproportionation process. An infrared absorption at 2100 cm^{-1}, indicative of *fac*-$[RuI_3(CO)_3]^-$,[16] was detected in these mixtures, and other related iodide complexes may be present as well.

$$\underset{\mathbf{7c}}{[Ru_3(\mu_3\text{-}I)(CO)_9]^-} \xrightarrow[\text{16 h}]{\text{100 °C}} \underset{\mathbf{10}\ (68\%)}{[Ru_6(CO)_{18}]^{2-}} + \ldots \tag{8}$$

When solutions of $Ru_3(CO)_{12}$ and iodide salts, which initially produce **3c** and then **7c**, were heated under N_2 to ~140 °C, the known cluster $[Ru_6C(CO)_{16}]^{2-}$ (**11**)[20] was formed in 67% yield. This product has been previously obtained by reduction of $Ru_3(CO)_{12}$ with $[Mn(CO)_5]^-$ in refluxing diglyme, a reaction that forms $[Ru_6(CO)_{18}]^{2-}$ at lower temperatures.[18a] Thus, this latter species must be an intermediate in both routes to the carbido complex. Indeed, isolated $[PPN]_2[Ru_6(CO)_{18}]$ has been shown to convert into $[PPN]_2[Ru_6C(CO)_{16}]$ upon heating.[21]

Reaction of $Fe_3(CO)_{12}$ with Iodide Salts. The carbonyl cluster $Fe_3(CO)_{12}$ has been reported to react with $[Et_4N]I$ to form $[Fe(CO)_4I]^-$ in low yield.[22] A reinvestigation of this reaction appeared warranted because of the poor yield and our quite different results in the $Ru_3(CO)_{12}$/iodide reactions. In addition, the reported IR spectrum of $[Fe(CO)_4I]^-$ (2062 (w), 2003 (s), 1975 (m) cm^{-1}) did not resemble, either in band positions or intensity ratios, the spectra of other $[Fe(CO)_4X]^-$ complexes. For example, $[Fe(CO)_4(CN)]^-$ has carbonyl absorptions at 2034 (m), 1946 (w), and 1927 (s) cm^{-1}.[23]

We have found that the reaction of $Fe_3(CO)_{12}$ with [PPN]I in dry THF at 65 °C yields two iron complexes. The minor fraction, a crystalline product isolated in 18% yield, has a color and IR spectrum corresponding to those originally reported for $[Et_4N][Fe(CO)_4I]$.[22] However, a closer examination of the IR spectrum reveals that this product is actually $[PPN][HFe_3(CO)_{11}]$,[24] and this formula is also supported by the elemental analyses. The hydride ligand may originate from traces of moisture in the solvent or from the methanol stabilizer present in commercial $Fe_3(CO)_{12}$. We suggest that the formation of $[HFe_3(CO)_{11}]^-$ occurs by a water gas shift like reaction involving the release of HI instead of H_2 (eq 9 and 10). Reaction 10 is

$$H_2O + I^- \rightleftharpoons HI + OH^- \tag{9}$$

$$Fe_3(CO)_{12} + OH^- \rightarrow [HFe_3(CO)_{11}]^- + CO_2 \tag{10}$$

a well-known process and has been used to prepare $[HFe_3(CO)_{11}]^-$,[25] and reaction 9 is a reasonable equilibria in a non-aqueous solvent such as THF. The HI formed in eq 9 could be expected to react with various species in solution to form oxidized iron iodide complexes.

The major product isolated from the reaction of $Fe_3(CO)_{12}$ with [PPN]I is authentic [PPN][Fe(CO)$_4$I] (**12**), and the dominant course of the reaction is that indicated in eq 11. Salt **12** has been characterized by elemental analysis and by its IR spectrum, which is similar to those of other $[Fe(CO)_4X]^-$ complexes.[23] A reaction

$$Fe_3(CO)_{12} + 3[PPN]I \xrightarrow[\text{THF}]{\text{67 °C, 1 h}} \underset{\mathbf{12}(38\%)}{3[PPN][Fe(CO)_4I]} \tag{11}$$

---

(14) (a) Laine, R. M.; Crawford, E. J. *J. Mol. Catal.* **1988**, *44*, 357. (b) Laine, R. M.; Wilson, R. B. *Aspects Homogeneous Catal.* **1984**, *5*, 217.

(15) (a) Johnson, B. F. G.; Lewis, J.; Raithby, P. R.; Suss-Fink, G. *J. Chem. Soc., Dalton Trans.* **1979**, 1356. (b) Keister, J. B. *J. Chem. Soc., Chem. Commun.* **1979**, 214. (c) For related reactions of $Ru_3(CO)_{12}$ with H_2 and NaOMe, see: Taube, D. J.; Rokicki, A.; Anstock, M.; Ford, P. C. *Inorg. Chem.* **1987**, *26*, 526.

(16) (a) Zoeller, J. R. *Inorg. Chem.* **1986**, *25*, 3933. (b) Colton, R.; Farthing, R. H. *Aust. J. Chem.* **1971**, *24*, 903.

(17) Macklin, P.; Geoffroy, G. L., to be submitted for publication.

(18) (a) Eady, C. R.; Johnson, B. F. G.; Lewis, J.; Malatesta, M. C.; Machin, P.; McPartlin, M. *J. Chem. Soc., Chem. Commun.* **1976**, 945. (b) Eady, C. R.; Jackson, B. F. G.; Lewis, J.; Malatesa, M. C.; McPartlin, M.; Nelson, W. J. H. *J. Chem. Soc., Dalton Trans.* **1980**, 383.

(19) (a) Eady, C. R.; Johnson, B. F. G.; Lewis, J. *J. Chem. Soc., Chem. Commun.* **1976**, 302. (b) John, G. R. Johnson, B. F. G.; Lewis, J.; Mann, A. L. *J. Organomet. Chem.* **1979**, *171*, C9.

(20) (a) Bradley, J. S.; Ansell, G. B.; Hill, E. W. *J. Organomet. Chem.* **1980**, *184*, C33. (b) Johnson, B. F. G.; Lewis, J.; Sankey, S. W.; Wong, K.; McPartlin, M.; Nelson, W. J. H. *J. Organomet. Chem.* **1980**, *191*, C3.

(21) Hayward, C. T.; Shapley, J. R. *Inorg. Chem.* **1982**, *21*, 3816.

(22) Abel, E. W.; Butler, I. S.; Jenkins, C. R. *J. Organomet. Chem.* **1967**, *8*, 382.

(23) (a) Ruff, J. K. *Inorg. Chem.* **1969**, *8*, 86. (b) Goldfield, S. A.; Raymond, K. N. *Inorg. Chem.* **1974**, *13*, 770.

(24) Isaacs, E. E.; Graham, W. A. G. *J. Organomet. Chem.* **1975**, *85*, 237.

(25) McFarlane, W.; Wilkinson, G. *Inorg. Synth.* **1966**, *8*, 198.

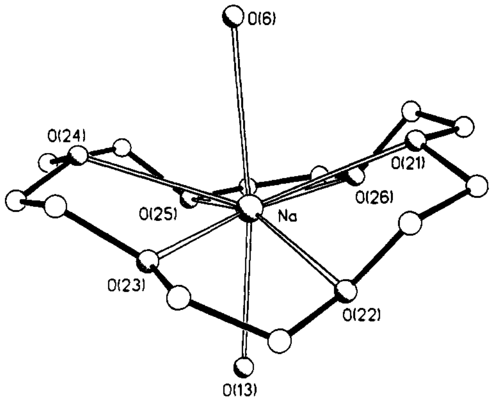

Figure 2. Structure of the $[Na(18\text{-crown-}6)]^+$ counterion, showing an unusual saddle-like distortion of the (gauche-anti-anti)$_6$ ring conformation.

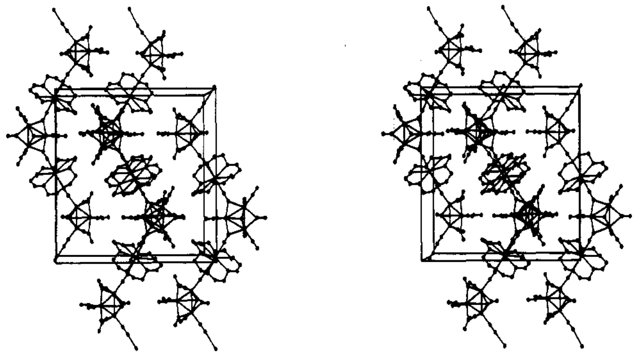

Figure 3. Stereo packing diagram of $[Na(18\text{-crown-}6)][Ru(\mu_3\text{-}I)(CO)_9]$ down the *c* axis (*b* vertical) showing the zigzag extended array along the *b* axis and the crystallographic mirror planes perpendicular to the *b* axis at $b = {}^1/_4$ and ${}^3/_4$.

between $Fe_3(CO)_{12}$ and [PPN]I in THF at 65 °C under 1 atm of H_2 gave the same relative amounts of $[PPN][HFe_3(CO)_{11}]$ and $[PPN][Fe(CO)_4I]$ as the reaction under N_2; hydrogen activation does not appear to be a significant process under these conditions.

Crystallographic Characterization of $[Na(18\text{-crown-}6)][Ru_3(\mu_3\text{-}I)(CO)_9]$ (7c). The cluster crystallizes in the orthorhombic space group *Pnma*, and as illustrated in Figure 1, the asymmetric unit consists of two half-formulas of $[Ru_3(\mu_3\text{-}I)(CO)_9]^-$, a $[Na(18\text{-crown-}6)]^+$ cation, and a half-molecule of CH_2Cl_2 (not shown) for each ion pair. Figure 2 shows an expanded view of the $[Na(18\text{-crown-}6)]^+$ cation, and the packing diagram in Figure 3 illustrates the zigzag extended ion-paired array that the compound adopts in the solid state. As illustrated in Figure 1, the cluster anion consists of a triangular Ru_3 core capped by a triply bridging iodide ligand. Each Ru atom bears two terminal CO's, and each Ru-Ru bond is bridged by a CO ligand. The sodium ion is coordinated by six oxygen atoms, four from the 18-crown-6 molecule and two from the cluster CO's. One of these CO's is a bridging CO for one cluster unit and the other is a terminal Ru–CO ligand. The arrangement is such that two terminal CO's of one $[Ru_3(\mu_3\text{-}I)(CO)_9]^-$ cluster anion are coordinated to Na^+ ions while two bridging CO's of the next cluster anion in the zigzag array coordinate to the cation.

Although there are minor differences in the Ru–Ru and the Ru–I bond lengths, the cluster anion is best described as an equilateral triangle of metal atoms symmetrically capped by the iodide ligand. The Ru–Ru distances average 2.756 Å, which is only slightly shorter than the benchmark Ru–Ru distance of 2.854 Å found in $Ru_3(CO)_{12}$.[26] The Ru–I distances average 2.782 Å and compare well to the average Ru–I distances of 2.685 Å in $HRu_3(\mu_3\text{-}I)(CO)_{10}$.[8] The similar Ru–Ru and Ru–I distances make the Ru_3I core of the cluster a nearly perfect tetrahedron as also reflected in the intercore angles, which show a maximum deviation of only 0.7° from the perfect tetrahedral angle of 60°.

The axially coordinated $[Na(18\text{-crown-}6)]^+$ complex contained in the structure of **7c** is highly and irregularly distorted, as shown in Figure 2. The "ideal" D_{3d} symmetry of $[K(18\text{-C-}6)]^+$ commonly distorts when a smaller Na^+ replaces K^+;[27] a folding inward of the polyether to maintain $Na^+\cdots$ether contacts is evident in Figure 2. The two carbonyl groups that adopt axially coordinated positions do so at very different distances: the Na–O(6) distance is 2.80 (2) Å, and Na–O(13) is 2.48 (2) Å. The values bracket the range in the Na–ether distances, 2.54 (3)–2.68 (2) Å. In line with the general observation that s character and basicity are inversely related,[28] the nominally sp^2 oxygen O(13) of the μ-CO should be a stronger donor than the terminal sp oxygen, O(6). Why both clusters do not use μ-CO groups to bind to Na^+ seems to result from restrictions to full eight-coordination by the ruffling of the macrocycle, which restricts access primarily in directions from which O(6) approaches (best seen in Figure 3). Thus, a strong interaction occurs for one of the carbonyl groups and favors a μ-CO over a terminal CO, while the long contact is of minimal importance. The essentially seven-coordinate complex that results is best described as a monocapped, trigonal prism with O(13) capping the square face formed by O(22), O(23), O(25), and O(26).

Concluding Remarks

The results reported herein, coupled with those described earlier by Kaesz and co-workers,[7,8] present a nearly complete picture of the equilibria that are present in solutions of $Ru_3(CO)_{12}$ containing halide ions. In this work we have provided spectroscopic data for the clusters **2a**, **2b**, **3b**, **3c**, and **6b**, have prepared and crystallographically characterized the new cluster $[Ru_3(\mu_3\text{-}I)(CO)_9]^-$ (**7c**), and have shown that clusters **3a**,**b** and **6a**,**b** as well as **3c** and **7c** readily interconvert through the addition and elimination of CO. In $Ru_3(CO)_{12}$ solutions containing chloride or bromide ions, clusters **2**, **3**, and **6** can form, with the equilibria dependent upon the CO partial pressure. In the absence of CO, the reactions proceed to form the tetranuclear butterfly clusters, although the **3** → **6** conversion is relatively slow at 22 °C. Under 1 atm of CO pressure, the equilibria shift completely to the left such that only cluster **2** can be detected. In $Ru_3(CO)_{12}$ solutions containing iodide ion, in the absence of a hydrogen source, only clusters **3c** and **7c** are formed (Scheme I), with **3c** produced when an atmosphere of CO is present and **7c** generated in the absence of CO.

The $Ru_3(CO)_{12}$/iodide system has been further investigated under H_2 and H_2/CO atmospheres, conditions appropriate for many reactions of catalytic interest.[1-5] Here the dominant reaction is iodide-induced disproportionation of $Ru_3(CO)_{12}$ into $[RuI_3(CO)_3]^-$ and $[HRu_3(CO)_{11}]^-$. This is an interesting combination of complexes, since $[HRu_3(CO)_{11}]^-$ is an effective hydride-transfer and reducing agent whereas $[RuI_3(CO)_3]^-$ has CO ligands bound to a formal Ru(II) center, which are thereby relatively susceptible to nucleophilic attack and reduction. It has been suggested that this combination of complexes may account for the CO reduction chemistry observed in $Ru_3(CO)_{12}$ solutions containing iodide ion under high synthesis gas pressure.[6]

It is anticipated that the results presented herein may prove generally useful to workers studying halide-promoted catalytic reactions of $Ru_3(CO)_{12}$.[1-5] A qualitative understanding of the equilibria present in $Ru_3(CO)_{12}$/halide solutions has now been achieved, but it is also desirable to have accurate equilibrium constants for these reactions under various temperature/pressure conditions. Such experiments appear feasible for those workers with appropriate instrumentation and interest since the equilibria are quite clean and are rapidly achieved.

Experimental Section

General Data. The salts [PPN]I and [PPN]Br were prepared from [PPN]Cl and the appropriate alkali-metal halide by precipitation from

---

(26) Churchill, M. R.; Hollander, F. J.; Hutchinson, J. P. *Inorg. Chem.* **1977**, *16*, 2655.

(27) Dale, J. *Isr. J. Chem.* **1980**, *20*, 3.

(28) Huheey, J. E. *Inorganic Chemistry*, 3rd ed.; Harper and Row: New York, 1983; p 150.

H_2O and were recrystallized from acetone–diethyl ether. The clusters $[PPN][Ru_4(\mu_2\text{-}Cl)(CO)_{13}]$[9] and $Ru_3(CO)_{12}$[16] were prepared according to the literature and $Fe_3(CO)_{12}$ (5-10% CH_3OH) was purchased and used as received. Solvents were dried by standard procedures, and all reactions were performed under dry N_2, H_2, or CO/H_2 atmospheres by using standard Schlenk techniques. Reactions at pressures above atmospheric were carried out in either glass pressure bottles (Fischer and Porter Co., Warminster, PA) or in a 200-mL Parr pressure reactor. Infrared spectra were recorded on Perkin-Elmer 281B and IBM FTIR-32 spectrophotometers using 0.1-mm NaCl and CaF_2 cells. Elemental analyses were performed by Galbraith Laboratories, Inc., Knoxville, TN, and Schwartzkopf Microanalytical Laboratories, Woodside, NY.

In Situ Formation of $[PPN][Ru_3(X)(CO)_{11}]$ (2a, X = Cl; 2b, X = Br). To a solution of $Ru_3(CO)_{12}$ (50 mg, 0.078 mmol) in THF (40 mL) was added 1 equiv of the appropriate [PPN]X salt, followed by stirring under N_2 for 2 h at 22 °C. During this time the orange solutions become burgundy red as **2a** and **2b** were formed. IR analysis indicated complete conversion to these species, but all attempts to isolate them by solvent evaporation led to CO loss and to the formation of **3a** and **3b**.

Preparation of $[PPN][Ru_3(\mu_2\text{-}X)(CO)_{10}]$ (3a, X = Cl; 3b, X = Br; 3c, X = I). Complexes **3a** and **3b** were generated by purging solutions of **2a** and **2b**, prepared as above, with N_2 for 40 min. During this time the color changed to an even darker red. Cluster **3c** immediately formed when [PPN]I was added to THF solutions of $Ru_3(CO)_{12}$. Dark red solid samples of **3a–c** were obtained by solvent evaporation followed by recrystallization from CH_2Cl_2/diethylether. However, satisfactory analyses were not obtained due to the partial conversion of **3a** and **3b** to **6a** and **6b** and **3c** to **7c** during this procedure. The presence of these impurities was indicated by IR analysis of the solid samples of **3a–c**.

Preparation of $[PPN][Ru_4(\mu_2\text{-}Br)(CO)_{13}]$ (6b). A solution of $Ru_3(CO)_{12}$ (1.28 g, 2.0 mmol) and [PPN]Br (1.24 g, 2.0 mmol) in THF (120 mL) was allowed to reflux under N_2 for 1 h. The solution was evaporated to dryness, and the residue was dissolved in a mixture of CH_2Cl_2 (5 mL) and Et_2O (25 mL). Hexane (50 mL) was added, and the solution was cooled to −35 °C for 17 h. The precipitate was collected and dried under high vacuum to yield **6b** as a microcrystalline solid (1.84 g, 66%). Anal. Calcd for $C_{49}H_{30}BrNO_{13}P_2Ru_4\cdot C_6H_{14}$ (hexane solvate): C, 44.84; H, 2.99; N, 0.95; Ru, 27.44; Br, 5.43. Found: C, 45.18; H, 2.72; N, 1.14; Ru, 27.67; Br, 4.27.

Preparation of $[PPN][Ru_3(\mu_3\text{-}I)(CO)_9]$ (7c). A solution of $Ru_3(CO)_{12}$ (3.84 g, 6.0 mmol) and [PPN]I (3.99 g, 6.0 mmol) in THF (360 mL) was allowed to reflux under N_2 for 1 h. The dark red solution was then evaporated to dryness, and the residue was dissolved in a mixture of CH_2Cl_2 (10 mL) and Et_2O (50 mL). Hexane (100 mL) was added, and the solution was cooled to −35 °C for 17 h. The precipitate was collected and dried under high vacuum to yield **7c** as a microcrystalline dark red solid (6.60 g, 95%). Anal. Calcd for $C_{45}H_{30}INO_9P_2Ru_3$: C, 44.26; H, 2.46; P, 5.08; N, 1.15; Ru, 25.08; O, 11.80; I, 10.40. Found: C, 44.86; H, 2.58; P, 5.28; N, 1.18; Ru, 26.03; O, 9.57; I, 10.68.

Protonation of 7c To Form $HRu_3(\mu_3\text{-}I)(CO)_9$ (5c). Cluster **7c** (95 mg, 0.078 mmol) was dissolved in THF (40 mL), and the solution was cooled to −78 °C. $HBF_4\cdot Et_2O$ was slowly added until the IR bands of **7c** completely disappeared as the color changed from red to orange. The solvent was removed by rotary evaporation, and the residue was extracted with Et_2O. After evaporation of the Et_2O, the orange solid was sublimed at 70 °C (10^{-2} mmHg) to give **5c** in 60% yield (32 mg). IR monitoring showed that addition of Et_3N to THF solutions of **5c** gave immediate deprotonation to form **7c**.

Preparation of $[PPN][RuI_3(CO)_3]$ (9). To a solution of $Ru_3(CO)_{12}$ (1.28 g, 2.0 mmol) and [PPN]I (3.99 g, 6.0 mmol) in THF (75 mL) was added HI (2.69 g of a 57% aqueous solution, 12.0 mmol) dropwise from an addition funnel followed by stirring for 2 h at 25 °C. The solution was then evaporated to dryness under vacuum, and the residue was dissolved in CH_2Cl_2 (30 mL) and diluted with Et_2O (90 mL). The solution was cooled to −35 °C for 40 h to give a crystalline product of **9**, which was dried under high vacuum (6.26 g, 95%). Anal. Calcd for $C_{39}H_{30}I_3NO_3P_2Ru$: C, 42.39; H, 2.72; N, 1.27. Found: C, 42.80; H, 2.98; N, 1.25.

Preparation of $[Et_3NH][HRu_3(CO)_{11}]$ (8). A solution of $Ru_3(CO)_{12}$ (6.24 g, 9.0 mmol) and NEt_3 (0.90 g, 9.0 mmol) in THF (150 mL) was allowed to reflux for 4.5 h while a stream of H_2 was passed through the mixture. The resulting dark red solution was filtered and evaporated to dryness under vacuum. The residue was then dissolved in a mixture of CH_2Cl_2 (20 mL) and diethyl ether (100 mL), filtered, diluted with hexane (140 mL), and cooled to −30 °C for 65 h. The resultant crystalline product **8** was dried under high vacuum (5.29 g, 82%). Anal. Calcd for $C_{17}H_{17}NO_{11}Ru_3$: C, 28.57; H, 2.38; N, 1.96. Found: C, 28.06; H, 2.39; N, 1.89.

Reaction of $Ru_3(CO)_{12}$ with [PPN]I in the Presence of H_2. A solution of $Ru_3(CO)_{12}$ (1.28 g, 2.0 mmol) in THF (150 mL) was allowed to stir for 1.5 h under 30 psig of H_2/CO at 65 °C. The solution was then evaporated to dryness, and the residue was extracted with Et_2O. The combined extracts were cooled to −35 °C for 17 h to give precipitation of the $[PPN][RuI_3(CO)_3]$ (**9**), which was dried under high vacuum (0.33 g, 35%). The remaining solution was concentrated under vacuum to yield $[PPN][HRu_3(CO)_{11}]$ (**8**) (1.62 g, 81%). The known complexes **8** and **9** were identified by their characteristic IR spectral data (Table I).

Table II. Crystal, Data Collection, and Refinement Data for $[Na(18\text{-crown-}6)][Ru_3(\mu_3\text{-}I)(CO)_9]$

(a) Crystal Data			
formula	$[Na(C_{12}H_{24}O_6)][Ru_3(CO)_9I]\cdot 0.5CH_2Cl_2$	V, Å^3	6634 (2)
		Z	8
fw	1011.95	μ, Mo Kα	24.0
cryst syst	orthorhombic	D(calcd), g cm^{-3}	2.026
space group	*Pnma*	cryst color	red
a, Å	20.214 (5)	cryst dimens, mm	0.21 × 0.23 × 0.40
b, Å	21.592 (6)		
c, Å	15.199 (3)	temp, K	294 (1)
(b) Data Collection			
diffractometer	Nicolet R3m/μ	no. of reflcns collcd	5258
radiation	MoKα	no. of indep reflcns	4879
wavelength, Å	λ = 0.71073	no. of obsd reflcns ($4\sigma F_o$)	2879
monochromator	graphite		
2θ limits, deg	$4 \leq 2\theta \leq 45$	std reflcns	3 std/197 reflcns
octants collcd	$+h,+k,+l$	decay	<2%
		T_{max}/T_{min}	0.192/0.151
(c) Refinement			
$R(F)$,[a] %	7.92	Δ/σ(final)	0.054
$R_w(F)$,[a] %	8.92	Δ/ρ(max), e Å^{-3}	1.48
GOF[b]	1.76		

[a] $R(F) = \sum(|F_o| - |F_c|)/\sum|F_o|$; $R_w(F) = \sum(w^{1/2}(|F_o| - |F_c|))/(w^{1/2}|F_o|)$.
[b] $GOF = [\sum w||F_o| - |F_c||/N_o - N_v]^{1/2}$.

Formation of $[PPN]_2[Ru_6(CO)_{18}]$ (10) upon 120 °C Thermolysis of $Ru_3(CO)_{12}$ in the Presence of [PPN]I. A solution of $Ru_3(CO)_{12}$ (2.0 g, 3.13 mmol) and [PPN]I (3.2 g, 4.81 mmol) in chlorobenzene (100 mL) was stirred under N_2 at 120 °C for 16 h. After the solution was cooled to 25 °C, diethyl ether (120 mL) was added. The mixture was cooled to −35 °C for 16 h to give a dark precipitate, which was recrystallized from chlorobenzene–Et_2O and dried under high vacuum to yield **10** in 68% yield (2.34 g). Anal. Calcd for $C_{90}H_{60}N_2O_{18}P_4Ru_6$: C, 49.41; H, 2.74; N, 1.28; P, 5.67. Found: C, 49.52; H, 2.79; N, 1.21; P, 5.12.

Formation of $[PPN]_2[Ru_6C(CO)_{16}]$ (11) upon 140 °C Thermolysis of $Ru_3(CO)_{12}$ in the Presence of [PPN]I. A solution of $Ru_3(CO)_{12}$ (3.0 g, 4.69 mmol) and [PPN]I (4.0 g, 6.02 mmol) in 1-methyl-2-pyrrolidinone (100 mL) was allowed to reflux under N_2 for 3 h. The solution was cooled, diluted with CH_2Cl_2 (150 mL), and washed with degassed H_2O (6 × 100 mL). The red-orange solution was concentrated to 30 mL under vacuum, and a mixture of hexane and Et_2O was added. When the solution was cooled to −35 °C for 96 h, a microcrystalline solid deposited, which was washed with Et_2O and dried under high vacuum to give the known cluster **11** in 67% yield (3.35 g).

Preparation of $[PPN][Fe(CO)_4I]$ (12) and $[PPN][HFe_3(CO)_{11}]$ (13). A solution of $Fe_3(CO)_{12}$ (5–10% MeOH, 2.0 g, ca. 3.6 mmol) and [PPN]I (8.12 g, 12.21 mmol) in THF (100 mL) was allowed to reflux under N_2 for 1 h. The solution was cooled to 25 °C, filtered, and evaporated to dryness. The residue was extracted repeatedly with diethyl ether, and the combined extracts were concentrated to 50 mL and diluted with hexane (100 mL). This mixture was cooled to −35 °C for 17 h to give microcrystalline $[PPN][HFe_3(CO)_{11}]$ (**13**) (0.66 g, ca. 18%). The remaining residue was dissolved in THF (50 mL) and filtered through diatomaceous earth. The solvent was removed under vacuum to leave a residue consisting mainly of $[PPN][Fe(CO)_4I]$ (3.41 g, ca. 38%). IR (THF): 2018 m, 1948 w, 1921 s cm^{-1}. Anal. Calcd for $C_{40}H_{30}FeINO_4P_2$ (**12**): C, 57.62; H, 3.60; N, 1.68; I, 15.25; Fe, 6.72. Found: C, 57.12; H, 4.39; N, 1.60; I, 16.55; Fe, 5.01. Anal. Calcd for $C_{47}H_{31}Fe_3NO_{11}P_2$ (**13**): C, 55.57; H, 3.05; N, 1.38; Fe, 16.55. Found: C, 55.57; H, 3.33; N, 1.42; Fe, 16.12.

Catalysis of the Water Gas Shift Reaction by $Ru_3(CO)_{12}$/[PPN]I. To a THF solution of **3c** (0.078 mmol) was added excess H_2O followed by stirring under nitrogen at room temperature for 4 h. This gave **7c** and CO_2, which were characterized by IR analysis, and the latter was also characterized by high-resolution mass spectral analysis. For the catalytic reaction, $Ru_3(CO)_{12}$ (50 mg, 0.078 mmol) and [PPN]I (65 mg, 0.098 mmol) were dissolved in THF in a 200-mL Fischer-Porter bottle. The reactor was charged with 50 psi of CO and stirred while being heated to 100 °C with an oil bath. After 13 h, the reactor was cooled to room temperature, and the gases above the reaction were analyzed by gas chromatography (Carbosieve G, Supelco, 100/120 mesh, oven tempera-

Table III. Atomic Coordinates (×10^4) and Isotropic Thermal Parameters ($Å^2 \times 10^3$) for $[Na(18\text{-crown-}6)][Ru_3(\mu_3\text{-}I)(CO)_9]$

	x	*y*	*z*	*U*[a]
Ru(1)	1352 (1)	1860 (1)	6490 (2)	67.2 (9)*
Ru(2)	2230 (2)	2500	5465 (2)	69 (1)*
Ru(3)	670 (1)	2500	1224 (2)	43.1 (9)*
Ru(4)	1852.2 (9)	1860.2 (8)	1286 (1)	43.1 (6)*
I(1)	897 (1)	2500	5025 (2)	62.4 (9)*
I(2)	1510 (1)	2500	−235 (2)	55.1 (9)*
Cls[b]	3913 (13)	1910 (8)	9061 (16)	319 (16)*
Cs[b]	3385 (24)	2500	9123 (54)	331 (75)*
Na	87 (5)	175 (4)	2259 (6)	59 (4)*
O(1)	415 (17)	2500	7883 (18)	98 (13)*
O(2)	2156 (12)	1456 (11)	8038 (14)	122 (11)*
O(3)	3425 (13)	2500	6611 (23)	102 (14)*
O(4)	2997 (16)	2500	3776 (20)	107 (15)*
O(5)	2329 (10)	1050 (9)	5375 (13)	89 (9)*
O(6)	497 (12)	743 (10)	6702 (14)	120 (11)*
O(11)	29 (15)	2500	2918 (21)	97 (9)
O(12)	−644 (12)	2500	221 (20)	81 (13)*
O(13)	593 (8)	1074 (7)	1499 (12)	65 (7)*
O(14)	2569 (11)	762 (9)	490 (16)	108 (10)*
O(15)	3191 (11)	2500	1506 (18)	67 (10)*
O(16)	2041 (11)	1422 (9)	3145 (12)	93 (9)*
O(21)	−483 (15)	−685 (11)	1256 (15)	131 (13)*
O(22)	−899 (11)	508 (11)	1178 (16)	109 (10)*
O(23)	−752 (14)	961 (12)	2802 (16)	121 (12)*
O(24)	189 (13)	448 (10)	3957 (14)	109 (11)*
O(25)	1275 (11)	118 (11)	2856 (13)	111 (10)*
O(26)	823 (15)	−591 (14)	1464 (20)	163 (15)*
C(1)	743 (27)	2500	7190 (31)	107 (22)*
C(2)	1820 (14)	1609 (14)	7437 (20)	82 (12)*
C(3)	2964 (22)	2500	6184 (26)	65 (11)
C(4)	2662 (18)	2500	4375 (22)	60 (14)*
C(5)	2129 (12)	1531 (15)	5579 (20)	84 (13)*
C(6)	808 (16)	1176 (13)	6644 (17)	79 (12)*
C(11)	211 (21)	2500	2199 (28)	71 (12)
C(12)	−153 (25)	2500	639 (20)	61 (16)*
C(13)	851 (10)	1534 (10)	1373 (13)	39 (7)*
C(14)	2333 (12)	1160 (11)	781 (18)	61 (10)*
C(15)	2648 (16)	2500	1441 (21)	48 (9)
C(16)	1974 (11)	1593 (11)	2392 (15)	50 (6)
C(21)	−49 (19)	−1077 (18)	862 (22)	125 (18)*
C(22)	−954 (18)	−492 (19)	629 (20)	123 (19)*
C(23)	−1312 (19)	27 (18)	1041 (33)	154 (24)*
C(24)	−1200 (16)	1024 (16)	1496 (25)	128 (19)*
C(25)	−1301 (18)	1124 (23)	2408 (30)	169 (27)*
C(26)	−790 (16)	966 (22)	3740 (20)	129 (20)*
C(27)	−179 (22)	985 (19)	4162 (28)	144 (22)*
C(28)	851 (19)	496 (19)	4274 (22)	158 (22)*
C(29)	1256 (23)	39 (18)	3760 (23)	151 (24)*
C(30)	1674 (18)	−283 (21)	2377 (36)	160 (27)*
C(31)	1431 (20)	−606 (30)	1764 (29)	235 (37)*
C(32)	540 (21)	−1158 (18)	1325 (26)	166 (25)*

[a] An asterisk denotes the equivalent isotropic *U* defined as one-third of the trace of the orthogonalized $\mathbf{U}_{ij}$ tensor. [b] Solvent molecule.

ture 30–200 °C, external standard method), which showed the formation of CO_2 with a turnover frequency of 5/day/Ru atom.

Crystallographic Analysis of $[Na(18\text{-crown-}6)][Ru_2(\mu_3\text{-}I)(CO)_9]$. The $[Na(18\text{-crown-}6)]^+$ salt of $[Ru_3(\mu_3\text{-}I)(CO)_9]^-$ was prepared analogously to the $[PPN]^+$ salt described above, except that NaI in the presence of 18-crown-6 was used in place of [PPN]I. The IR spectra of the two salts in CH_2Cl_2 solutions were identical. Red crystals of $[Na(18\text{-crown-}6)][Ru_3(\mu_3\text{-}I)(CO)_9]$ were obtained by slow diffusion of hexane into CH_2Cl_2 solutions of the compound. All specimens examined showed weak and diffuse diffraction typical of oddly shaped ionic compositions, which limited data collection to $2\theta \le 45°$. Table II summarizes the experimental parameters. Systematic absenses in the diffraction data and photographic evidence limited the possible space groups to the orthorhombic settings $Pn2_1a$ (nonstandard $Pna2_1$) or *Pnma*. The latter, centrosymmetric, choice was initially suggested by the *E* statistics and was confirmed by the presence of crystallographic *m* symmetry and the computationally stable and chemically reasonable results of refining this model. The asymmetric unit consists of two half-formulas of $[Ru_3(\mu_3\text{-}I)(CO)_9]^-$, a $[Na(18\text{-crown-}6)]^+$ cation, and a half-molecule of CH_2Cl_2 for each ion pair. The data were empirically corrected for absorption and for a 2% linear decay in intensity.

Table IV. Selected Bond Distances (Å) and Angles (deg) for $[Na(18\text{-crown-}6)][Ru_3(\mu_3\text{-}I)(CO)_9]$

(a) Ru–Ru			
Ru(1)–Ru(2)	2.737 (4)	Ru(3)–Ru(4)	2.761 (3)
Ru(1)–Ru(1a)	2.764 (4)	Ru(4)–Ru(4a)	2.763 (4)
Ru(2)–Ru(1)–Ru(1a)	59.7 (1)	Ru(4)–Ru(3)–Ru(4a)	60.0 (1)
Ru(1)–Ru(2)–Ru(1a)	60.7 (1)	Ru(3)–Ru(4)–Ru(4a)	60.0 (1)
(b) Ru–I			
Ru(1)–I(1)	2.778 (3)	Ru(3)–I(2)	2.793 (4)
Ru(2)–I(1)	2.776 (4)	Ru(4)–I(2)	2.781 (3)
Ru(1)–I(1)–Ru(1a)	59.7 (1)	Ru(3)–I(2)–Ru(4)	59.4 (1)
Ru(1)–I(1)–R1(2)	59.1 (1)	Ru(4)–I(2)–Ru(4a)	59.6 (1)
I(1)–Ru(1)–Ru(2)	60.4 (1)	I(2)–Ru(3)–Ru(4)	60.1 (1)
I(1)–Ru(1)–Ru(1a)	60.2 (1)	I(2)–Ru(4)–Ru(3)	60.5 (1)
I(1)–Ru(2)–Ru(1)	60.5 (1)	I(2)–Ru(4)–Ru(4a)	60.2 (1)
(c) Ru–CO			
Ru(1)–C(1)	2.13 (4)	Ru(3)–C(11)	1.75 (4)
Ru(1)–C(2)	1.81 (3)	Ru(3)–C(12)	1.89 (4)
Ru(1)–C(5)	2.21 (3)	Ru(3)–C(13)	2.13 (2)
Ru(1)–C(6)	1.86 (3)	Ru(4)–C(13)	2.15 (2)
Ru(2)–C(3)	1.84 (4)	Ru(4)–C(14)	1.95 (3)
Ru(2)–C(4)	1.87 (3)	Ru(4)–C(15)	2.13 (2)
Ru(2)–C(5)	2.11 (3)	Ru(4)–C(16)	1.79 (2)
Ru(1)–C(1)–Ru(1a)	81 (2)	Ru(3)–C(13)–Ru(4)	80.4 (8)
Ru(1)–C(5)–Ru(2)	79 (1)	Ru(4)–C(15)–Ru(4a)	80.7 (12)
Ru(1)–C(1)–O(1)	137 (1)	Ru(3)–C(13)–O(13)	143 (2)
Ru(1)–C(5)–O(5)	135 (2)	Ru(4)–C(13)–O(13)	137 (2)
Ru(2)–C(5)–O(5)	147 (2)	Ru(4)–C(15)–O(15)	139.6 (6)
(d) $Na[18\text{-crown-}6]^+$			
Na–O(6)	2.80 (2)	Na–O(23)	2.54 (3)
Na–O(13)	2.48 (2)	Na–O(24)	2.66 (2)
Na–O(21)	2.67 (3)	Na–O(25)	2.57 (2)
Na–O(22)	2.68 (2)	Na–O(26)	2.53 (3)
C(6)–O(6)–Na	150 (2)	C(13)–O(13)–Na	162 (2)
O(6)–Na–O(13)	173.0 (7)		

The structure was solved by direct methods and completed by subsequent difference Fourier syntheses. All non-hydrogen atoms were refined anisotropically and hydrogen atoms were treated as idealized, updated isotropic contributions (*d*(CH) = 0.96 Å). Atomic coordinates are given in Table III; bond distances and angles are given in Table IV. SHELXTL (5.1) software was used for all computations and served as the source for scattering factors (G. Sheldrick, distributed by Nicolet XRD, Madison, WI).

Acknowledgment. We thank the Department of Energy, Office of Basic Energy Sciences (G.L.G.), and Union Carbide Corp. (B.D.D.) for support of this research and the National Science Foundation for providing funds toward the purchase of the diffractometer at the University of Delaware. We also acknowledge G. Steinmetz, R. Hale, J. Blank, and R. Minard for obtaining mass spectra, C. P. Wolfe for excellent technical assistance, the Johnson Matthey Co. for a loan of precious metal salts, and W. L. Gladfelter, H. Kaesz, G. Lavigne, and N. Lugan for helpful discussions.

Supplementary Material Available: Tables of isotropic thermal parameters, complete bond lengths and angles, and calculated hydrogen atom positions (5 pages); a table of structure factors (16 pages). Ordering information is given on any current masthead page.